

## Optimization of Combustion Chamber for Diesel Engine Using Kriging Model\*

Shinkyu JEONG\*\* Youichi MINEMURA\*\* and Shigeru OBAYASHI\*\*

\*\*Institute of Fluid Science, Tohoku University,  
2-1-1 Katahira, Aoba-ku, Sendai, 980-8577, JAPAN  
E-mail: jeong@edge.ifs.tohoku.ac.jp

### Abstract

Diesel engine combustion chamber which reduces exhaust emission has been designed using CFD analysis and optimization techniques. In order to save computational time for design, the Kriging model, one of the response surface models, is adopted here. For a robust exploration, both the estimated function value of the model and its uncertainty are considered at the same time. In the present problem, the k-means method is used to limit the number of additional sample points to a reasonable level. Among the additional sample points, two combustion chamber shapes dominate the baseline configuration in terms of all objective functions. Compared with the previous optimization with the evolutionary algorithm, its computational time for design was cut by 95%. The results indicate that the present method is a practical approach for real-world applications.

**Key words:** Diesel Engine, Exhaust Emission Reduction, Kriging Model

### 1. Introduction

The market share for diesel car has increased in European countries because of its high thermal efficiency and low carbon dioxide emissions. The trend is expected to be continued in the future. However, the problems with diesel engine are its higher Particulate Matter (PM) and Nitrogen Oxide (NO<sub>x</sub>) emissions. The European environmental group demands more strict emission standard than now. EURO5, which will be applied from 2009, requires a further 80% reduction in PM and a further 20% reduction in NO<sub>x</sub>. In order to cope with this strict emission standard, green engine which reduces exhaust emission should be developed. Generally, NO<sub>x</sub> is produced when combustion occurs at high temperatures because the nitrogen contained in the combustion air will also react with the available oxygen, and soot is produced as a byproduct of incomplete combustion when oxygen is insufficient or temperature is too low. One idea of reducing NO<sub>x</sub> is to mix high temperature burn-gas with cold air in combustion chamber as quickly as possible, and cool down the local high temperature region, as shown in Fig. 1. By doing this, NO<sub>x</sub> emission can be reduced without any additional increase of soot. The mixture of burn-gas and cold air can be activated by generating a swirl flow in the combustion chamber. The flow in the combustion chamber largely depends on the shape of chamber. Consequently, the exhaust emission can be reduced effectively by designing the geometry of combustion chamber<sup>(1)</sup>. In this study, the combustion chamber of diesel engine is designed by using CFD analysis and optimization techniques. However, analysis of engine combustion using CFD requires a lot of computational time. It is not so efficient to couple the time-consuming CFD analysis code with evolutionary algorithm.

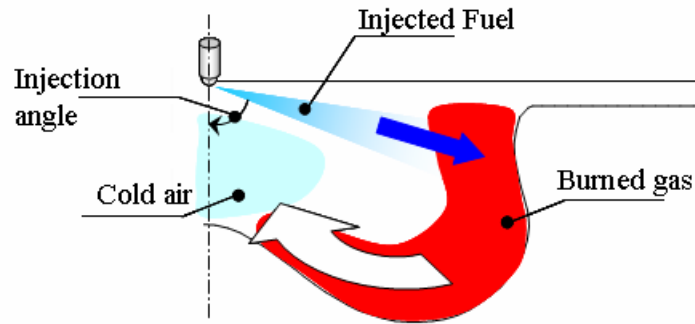


**Figure 1 NOx reduction mechanism**

For an efficient design, a Kriging model<sup>(2)</sup>, one of the Response Surface Models (RSM), is adopted for optimization. The Kriging model developed in the field of spatial statistics and geostatistics, and predicts not a functional value itself but the distribution of functional value at the unknown point. From this distribution, it is possible to predict both the function value and its uncertainty at the same time. The uncertainty information is very useful when using the RSM in optimization. One of the drawbacks of using RSM in optimization is that it is apt to miss the global optimum because estimation value obtained with RSM includes errors at an unknown point. By considering the estimated function value and its uncertainty simultaneously, robust exploration of the global optimum and improvement of the model are possible.<sup>(3)</sup> The method was successfully applied to single objective optimization design.<sup>(4), (5)</sup>

For the multi-objective problem, Knowles suggested ParEGO<sup>(6)</sup> (Pareto Efficient Global Optimization) which converts all objective functions into a single objective function by using a parameterized weighting vector. However, the result of utility function method largely depends on the weighting vector. The present author suggested EGOMOP<sup>(7)</sup> (Efficient Global Optimization for Multi-Objective Problem) in which each objective function is converted into its EI, and this value is used as fitness in multi-objective optimization problem. Furthermore, the k-means clustering method is adopted for the efficient selection of additional sample points in high dimensional problem. In this study, the optimization was performed with the following four objective functions: soot, NO, CO and thermal efficiency. Among the additional sample points, two solutions dominate the baseline configuration in terms of all objective functions. The results show the usefulness of the present method.

## 2. Kriging Model

The present Kriging model expresses the unknown function  $y(\mathbf{x})$  as:

$$y(\mathbf{x}) = \mu + Z(\mathbf{x}) \quad (1)$$

where  $\mathbf{x}$  is an  $m$ -dimensional vector ( $m$  design variables),  $\mu$  is a constant global model, and  $Z(\mathbf{x})$  represents a local deviation from the global model. In the model, the local deviation at an unknown point ( $\mathbf{x}$ ) is expressed using stochastic processes. Sample points are interpolated with the Gaussian random function as the correlation function to estimate the trend in the stochastic processes. The correlation between  $Z(\mathbf{x}^i)$  and  $Z(\mathbf{x}^j)$  is strongly related to the distance between the two corresponding points,  $\mathbf{x}^i$  and  $\mathbf{x}^j$ . In the Kriging model, a specially weighted distance is used instead of the Euclidean distance because the latter weighs all design variables equally. The distance function between the point at  $\mathbf{x}^i$  and  $\mathbf{x}^j$  is expressed as:

$$d(\mathbf{x}^i, \mathbf{x}^j) = \sum_{k=1}^m \theta_k |x_k^i - x_k^j|^2 \quad (2)$$

where  $\theta_k$  ( $0 \leq \theta_k \leq \infty$ ) is the  $k_{th}$  element of the correlation vector parameter,  $\theta$ . The correlation between the points,  $\mathbf{x}^i$  and  $\mathbf{x}^j$ , is defined as:

$$Corr[Z(\mathbf{x}^i), Z(\mathbf{x}^j)] = \exp[-d(\mathbf{x}^i, \mathbf{x}^j)] \quad (3)$$

The Kriging predictor is

$$\hat{y}(\mathbf{x}) = \hat{\mu} + \mathbf{r}'\mathbf{R}^{-1}(\mathbf{y} - \mathbf{1}\hat{\mu}) \quad (4)$$

where  $\hat{\mu}$  is the estimated value of  $\mu$ ,  $\mathbf{R}$  denotes the  $n \times n$  matrix whose  $(i, j)$  entry is  $Corr[Z(\mathbf{x}^i), Z(\mathbf{x}^j)]$ ,  $\mathbf{r}$  is the vector whose  $i_{th}$  element is

$$r_i(\mathbf{x}) \equiv Corr[Z(\mathbf{x}), Z(\mathbf{x}^i)] \quad (5)$$

and  $\mathbf{y} = [y(\mathbf{x}^1), \dots, y(\mathbf{x}^n)]$ , and  $\mathbf{1}$  denotes an  $n$ -dimensional unit vector.

The unknown parameter,  $\theta$ , for the Kriging model can be estimated by maximizing the following likelihood function:

$$Ln(\hat{\mu}, \hat{\sigma}^2, \theta) = -\frac{n}{2} \ln(\hat{\sigma}^2) - \frac{1}{2} \ln(|\mathbf{R}|) \quad (6)$$

Maximizing the likelihood function is an  $m$ -dimensional unconstrained non-linear optimization problem. In the present study, a genetic algorithm was adopted to solve this problem. For a given  $\theta$ ,  $\hat{\mu}$  and  $\hat{\sigma}^2$  can be defined as follows:

$$\hat{\mu} = \frac{\mathbf{1}'\mathbf{R}^{-1}\mathbf{y}}{\mathbf{1}'\mathbf{R}^{-1}\mathbf{1}} \quad (7)$$

$$\hat{\sigma}^2 = \frac{(\mathbf{y} - \mathbf{1}\hat{\mu})'\mathbf{R}^{-1}(\mathbf{y} - \mathbf{1}\hat{\mu})}{n} \quad (8)$$

The accuracy of the prediction value depends largely on the distance from sample points. Intuitively, the closer point  $\mathbf{x}$  is to the sample points, the more accurate the prediction,  $\hat{y}(\mathbf{x})$ , becomes. This is expressed in the following equation:

$$s^2(\mathbf{x}) = \hat{\sigma}^2 \left[ 1 - \mathbf{r}'\mathbf{R}^{-1}\mathbf{r} + \frac{(\mathbf{1} - \mathbf{1}\mathbf{R}^{-1}\mathbf{r})^2}{\mathbf{1}'\mathbf{R}^{-1}\mathbf{1}} \right] \quad (9)$$

where  $s^2(\mathbf{x})$  is the mean squared error at point  $\mathbf{x}$ , indicating the uncertainty of the estimated value.

### 3. Exploration of Optimum with Kriging model

Once the approximation model is constructed, the optimum can be explored using an arbitrary optimizer on the model. However, there is a possibility of missing the global optimum because the estimated value includes uncertainty in it.

In Fig. 2, the solid line represents the real shape of the objective function and the dotted line stands for the approximation model. The minimum point on the approximation model is located near  $x = 9$ , whereas, the real global minimum of the objective function is situated near  $x = 4$ . Exploration of the global minimum using the approximation model tends to result in the local minimum. For a robust search of the global optimum in the approximation model, the uncertainty information is very useful.

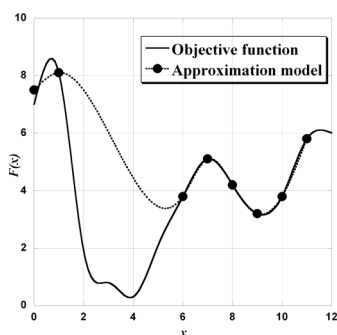


Figure 2 Real objective function and approximation model

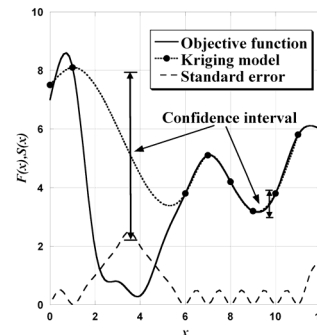


Figure 3 Estimated value and standard error model of Kriging model

Figure 3 shows the estimated value and the standard error (uncertainty) of the Kriging model. Around  $x = 9.5$ , the standard error of the Kriging model is very small because there are many sample points around this point. Consequently, the confidence interval is very small as shown in Fig. 3. On the other hand, the standard error around  $x = 3.5$  is very large due to the lack of sample points there. Consequently, the confidence interval at this point is very wide. The lower bound of this interval is smaller than the current minimum in the Kriging model. As a result, this point has some probability of being superior to the current minimum.

The probability of being superior to the current optimum can be expressed by the criterion of expected improvement (EI). In minimization problems, EI can be calculated as follows on the Kriging model:

$$I(x) = \begin{cases} [f_{\min} - y(x)] & \text{if } y(x) < f_{\min} \\ 0 & \text{otherwise} \end{cases} = \max(f_{\min} - y, 0) \quad (10)$$

$$E(I) = \int_{-\infty}^{f_{\min}} (f_{\min} - y)\phi(y)dy \quad (11)$$

where  $\phi$  is the probability density function representing uncertainty about  $y$ . By selecting the maximum EI point as additional sample points for the Kriging model iteratively, robust exploration of the global optimum is possible. The overall procedure is shown in Fig. 4.

1. Select initial sample points using arbitrary space filling method.
2. Construct Kriging model for an objective function.
3. Explore the maximum EI point using GA
4. Add the maximum EI point as an additional sample point
5. Iterate 2-4 until termination criterion (maximum number of sample points or tolerance of uncertainty) is met.

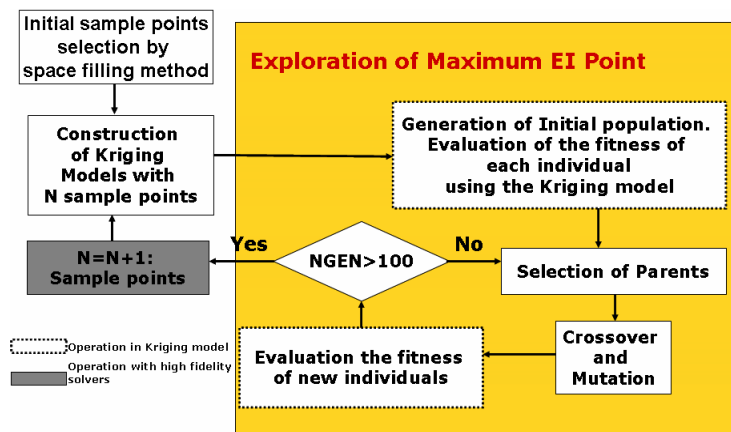


Figure 4 Procedure of optimization using the Kriging model

#### 4. Extension to multi-objective problem

In this study, EGOMOP (Efficient Global Optimization for Multi-Objective Problem) which converts each objective function into its EI, and uses these EIs as fitness of multi-objective optimization problem is applied. While the single objective problem obtains the maximum EI point, the multi-objective problem obtains the Pareto solutions of EIs. From these Pareto solutions, several points should be selected as additional sample points.

However, even if we select only extreme Pareto solutions and middle points, a number of additional sample points will grow increasingly in the case of high dimensional problems, as shown in Fig. 5.

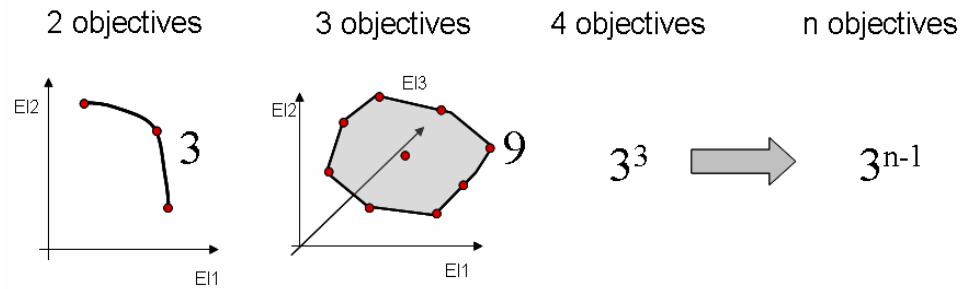


Figure 5 A number of additional sample points

In order to limit the number of additional sample points to a reasonable level, the k-means method<sup>(8)</sup>, one of the clustering methods<sup>(9)</sup> is adopted here. The k-means method groups all members into a given number of clusters based on the Euclidean distance. Once the clustering is over, centers of clusters are selected as additional sample points. The overall procedure of the present method is shown in Fig. 6.

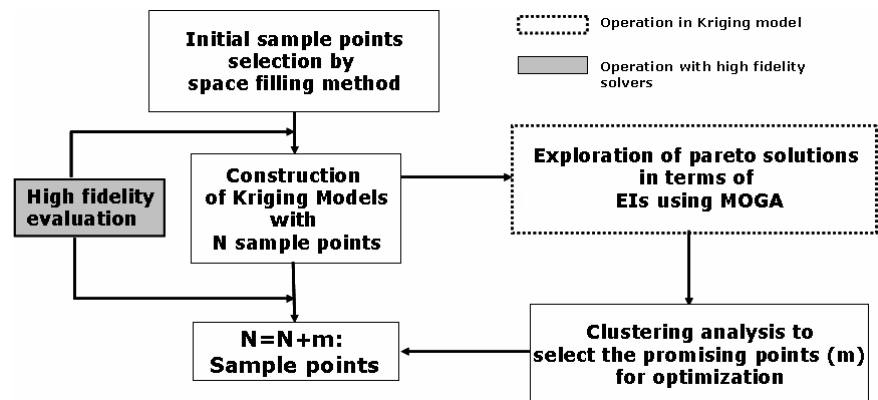


Figure 6 Overall procedure of the present method

#### 5. Results

##### 5.1 Definition of design problem and evaluation

The objective functions used in this study are as follows:

1. Soot minimization
2. Thermal NO minimization
3. CO minimization
4. Thermal efficiency maximization

The combustion chamber shape is a body of rotation and half of its cross-section is defined with 10 design variables as shown in Fig. 7. Injection angle is also defined as design variable because the diesel engine combustion largely depends on the injection angle. Detailed engine geometry and operating condition are shown in Table 1.

Table 1 Engine configuration and operating condition

Bore×Stroke	Φ86mm×86mm
Compression ratio	16.9
Nozzle type	Φ0.135×6 holes
Engine speed	2000rpm
Injection timing	315.1~318.2 (first) 362.1 ~372.3 (second)
Rail Pressure	98 MPa
Swirl ratio	2
EGR	25%

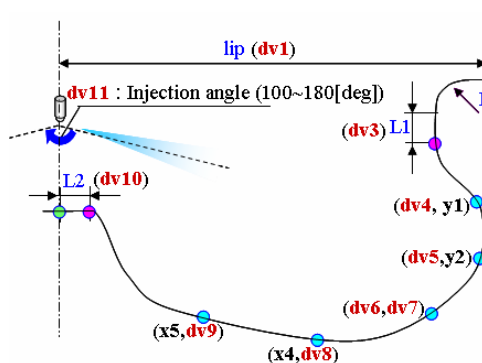


Figure 7 Definition of design variables

Under this condition, one full cycle, from  $180^\circ$  to  $450^\circ$  crank angles, is evaluated with GTT code developed by Wakisaka et al.<sup>(10)-(12)</sup> This code is based on the finite-volume method and boundary fitted grid, and takes into accounts the fluid flow, fuel spray, combustion, and so on. The spray model is based on the Discrete Droplet Model (DDM) and includes sub-models for break up, collision and merger. Ignition is achieved by Livengood integration<sup>(13)</sup>. In the combustion model, overall-reaction formula<sup>(14)</sup> associated with the equivalence ratio is used for gas composition calculation. The NO<sub>x</sub> model<sup>(15)</sup> dealing with thermal-NO and soot model<sup>(16)</sup> dealing with both formation and oxidation are also included. The validity of the GTT code has been confirmed by real engine designs in the industry.

## 5.2 Results of optimization

48 initial sample points are selected for construction of the Kriging model using the Latin Hypercube Sampling (LHS)<sup>(17)</sup>, and 6 iterations of design procedure shown in Fig. 6 are performed with 43 additional sample points. All sample points are projected onto the two-objective function planes in Fig. 8. Compared with the initial sample points, the additional sample points appear in the optimum direction. It means that the present algorithm works effectively. In Fig. 8, NO-CO, NO-Thermal efficiency shows the trade-off relation. Among 43 additional sample points, two solutions (Opt1 and Opt2) outperform the baseline configuration in terms of all objective functions. Temperature distribution of these two solutions is compared with that of the baseline configuration in Fig. 9. Compared with the baseline configuration, the lower center part of these solutions is more inflated towards the sidewall. It may push the cold air in the center of the combustion chamber to the wall side and generates a swirl flow. This swirl flow promotes a mixture of burn-gas and cold air and cools down the high temperature region. Consequently, this cooling effect reduces the exhaust emission. Iso-surfaces of soot and thermal NO emissions are shown in Fig. 10 and Fig. 11, respectively. Soot and thermal NO emissions of the designed configurations are less

than those of the baseline configuration. Table 2 shows the performance improvements of the designed combustion chambers. In this study, a total of 91 GTT evaluations were conducted. It is about one twentieth of the previous optimization using evolutionary algorithm with GTT evaluation.

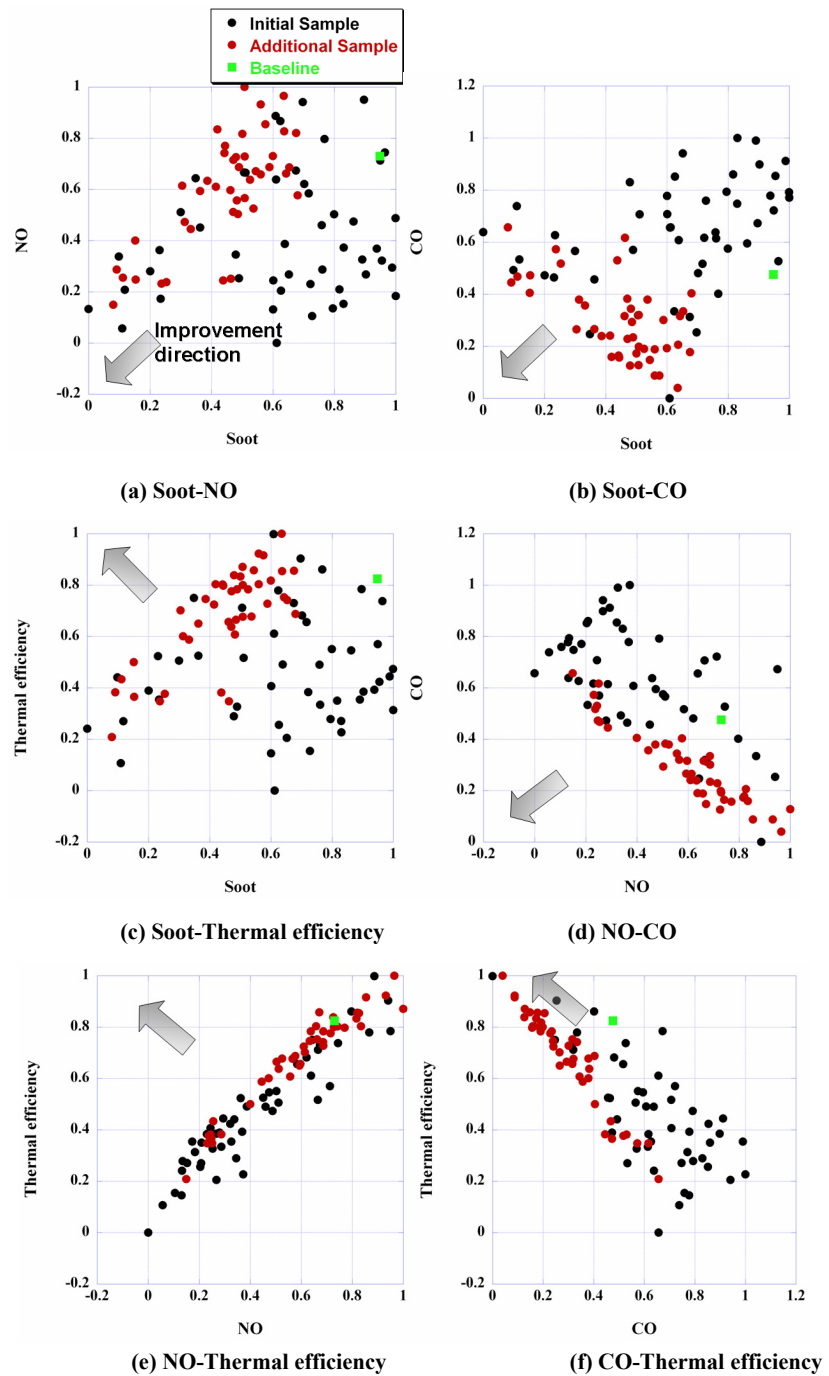


Figure 8 Projection of sample points onto two-objective planes

Table 2 Performance improvements to the baseline configuration

	Soot	NO	CO	Thermal efficiency
Opt. 1	17.98%	0.4277%	31.05%	0.63%
Opt. 2	15.49%	6.12%	29.09%	1.56%

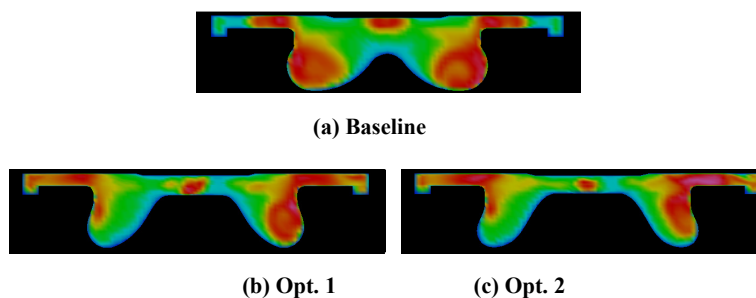


Figure 9 Comparison of temperature distributions

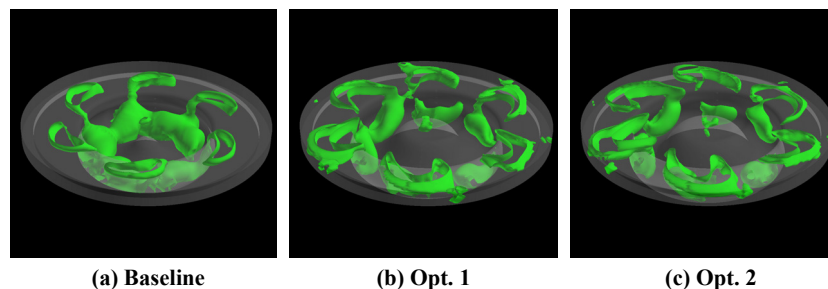


Figure 10 Comparison of iso-surfaces of soot

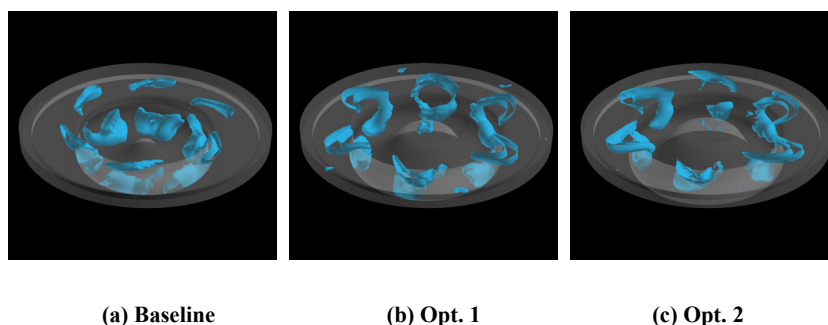


Figure 11 Comparison of iso-surfaces of thermal NO

## 6. Conclusions

In this study, diesel engine combustion chamber which reduces exhaust emission has been designed using CFD analysis and optimization techniques. In order to save the computational burden of optimization, the Kriging model, one of the response surface models, was adopted. The points which have a large probability of being optimum are estimated using the Kriging model, and used as additional sample points to update the Kriging model. For an efficient selection of additional sample points, the k-means method, one of the clustering techniques, was also used here. After 43 additional sample points are added, two solutions outperform the baseline configuration in terms of all objective functions. Compared with the previous optimization with the evolutionary algorithm, its computational time for design was reduced by 95%. The results indicate that the present method is a practical approach for real-world applications.

## References

- (1) D. Shimo, M. Kataoka and H. Fujimoto, "Effect of Cooling of Burned Gas by Vertical Vortex on NO<sub>x</sub> Reduction in Small DI Diesel Engines," SAE2004-01-0125, (2004).
- (2) J. Sack, W. J. Welch, T. J. Mitchell and H. P. Wynn, "Design and Analysis of Computer Experiments (with discussion)," Statistical Science, Vol.4 (1996), pp. 409-435.



- (3) R. J. Donald, S. Matthias and J. W. William, "Efficient Global Optimization of Expensive Black-Box Function," *Journal of Global Optimization.*, Vol.13 (1998), pp. 455-492.
- (4) A. J. Keane, "Wing Optimization Using Design of Experiment, Response Surface, and Data Fusing Methods," *Journal of Aircraft*, Vol.40 (2003), pp. 741-750.
- (5) S. Jeong, M. Murayama and K. Yamamoto, "Efficient Optimization Design Method Using Kriging Model," *Journal of Aircraft*, Vol.42 (2005), pp. 412-420.
- (6) Knowles, J. and Hughes, E. J., "Multiobjective Optimization on a Budget of 250 Evaluation," *Proceeding of third international conference of EMO (2005)*, pp. 176-190.
- (7) S. Jeong and S. Obayashi, "Efficient Global Optimization (EGO) for Multi-Objective Problem and Data Mining," *Proceeding of Congress on Evolutionary Computation*, Vol.3 (2005), pp. 2138-2145.
- (8) Y. Jin and B. Sendhoff, "Reducing Fitness Evaluation Using Clustering Techniques and Neural Network Ensembles," *Proceedings of Genetic and Evolutionary Computation Conference (2004)*, pp. 688-699.
- (9) A. K. Jain, M. N. Murty and P. J. FLYNN, "Data Clustering: A Review," *ACM Computing Surveys*, Vol. 31 (1999), pp. 264-323.
- (10) T. Wakisaka, Y. Shomatomo, Y. Isshiki, N. Sumi, K. Tanuma and R. M. Modien, "Analysis of the Effects of In-Cylinder Flows dueing Intake Storke on the Flow Characteristics near Compression TDC in Four-Stroke Cylce Engines," *Proceeding of COMODIA (1990)*, pp. 487-492.
- (11) T. Wakisaka, Y. Shimatomo, Y. Isshiki, T. Noda, A. Matsui and S. Akamatsu, "Numerical Analysis of Spray Phenomena in Fuel Injection Engines," *Proceeding of COMODIA (1994)*, pp. 403-409.
- (12) T. Wakisaka, S. Takeuchi, F. Imamura, K. Ibaraki and Y. Isshiki, "Numerical Analysis of Diesel Spray Impinging on Combustion Chamber Walls by Means of a Discrete Droplet / Liquid-Film Model," *Proceeding of COMODIA (1998)*, pp. 462-492.
- (13) J. C. Livengood and P. C. Wu, "Correlation of Autoignition Phenomena in Internal Combustion Engines and Rapid Compression Machines," *Proceeding of the Fifth International Symposium on Combustion (1955)*, 347-356.
- (14) T. Takagi, Y. Fukuyama, T. Okamoto and Y. Nakano, "Numerical Simulation of Mixing and Combustion in Transient Sprays," *Proceeding of COMODIA (1994)*, 397-402.
- (15) P. Eyzat and J. C. Guibet, "A New Look at Nitrogen Oxides Formation in Internal Combustion Engine," *SAE paper*, NO. 680124, (1968).
- (16) J. Nagle and R. F. Strickland-Constable, "Oxidation of Carbon between 1000-2000 Degree," *Proceeding of the Fifth Carbon Conference*, Vol. 1 (1962), 154-164.
- (17) M. D. Mckay, R. J. Beckman and W. J. Conover, "A Comparison of Three Methods for Selecting Values of Input Variables in the Analysis of Output from a Computer Code," *Technometric*, Vol. 21 (1979), 239-245.